Studies of the Ankyrin Repeats of the *Drosophila melanogaster* Notch Receptor. 1. Solution Conformational and Hydrodynamic Properties†

Mark E. Zweifel and Doug Barrick*

T. C. Jenkins Department of Biophysics, The Johns Hopkins University, 3400 North Charles Street, Baltimore, Maryland 21218

Received July 10, 2001

ABSTRACT: To gain insight into the structural basis for Notch signaling, and to investigate the relationship between structure and stability in ankyrin repeat proteins, we have examined structural features of polypeptides from the *Drosophila melanogaster* Notch protein that contain five, six, and a putative seventh ankyrin repeat. Circular dichroism (CD) spectroscopy indicates that Notch ankyrin polypeptides of different length contain a significant amount of α-helix, indicating that a folded structure can be maintained despite the loss of individual ankyrin modules. However, the α-helical content of the construct with the putative seventh repeat is slightly higher than polypeptides containing fewer repeats, suggesting that the putative seventh repeat may help stabilize other parts of the ankyrin domain. Fluorescence spectroscopy indicates that the single tryptophan in the fifth ankyrin repeat is in a nonpolar environment and is shielded from solvent in all three constructs, although slight differences in spectroscopic properties of the six- and five-repeat constructs are observed, indicating minor structural changes. Near-UV CD indicates that these ankyrin polypeptides contain a significant amount of fixed tertiary structure surrounding their aromatic side chains. Gel filtration chromatography and sedimentation equilibrium studies indicate that these ankyrin repeat polypeptides are monomeric. Sedimentation velocity studies indicate that each polypeptide exhibits significant axial asymmetry, consistent with the elongated structure seen for other for ankyrin repeat proteins. However, the degree of asymmetry is greatest for the construct containing six repeats, suggesting that in the absence of the putative seventh repeat, the sixth repeat is partly unfolded.

The Notch pathway is a ubiquitous transmembrane signaling pathway involved in a variety of cell-fate decisions in higher eukaryotes (*1*−*6*). Through extensive genetic studies, a large number of genes have been identified that specifically influence Notch signaling in *Drosophila melanogaster* (*7*−*9*) and *Caenorhabditis elegans* (*3, 10*). One of the central components in the Notch signaling pathway is the product of the Notch gene, a large (2703 residues in *Drosophila*), single-pass transmembrane receptor (*11, 12*). Signaling is initiated by binding of extracellular ligand to specific EGF-like repeats in the receptor (*13*−*15*), and is potentiated by one or more proteolytic cleavages (*16*−*20*) and by dissociation of receptor heterodimers on the extracellular side of the cell membrane (*21*). As a result of these extracellular and transmembrane modifications to the Notch receptor, the intracellular portion of the receptor (∼1000 residues in *D. melanogaster*) dissociates from the membrane, enters the nucleus, and activates transcription of downstream genes (*16, 17, 19*).

The activity of the cleaved, intracellular portion of the Notch receptor (termed NIC)[1] is modulated by a large number of proteins [reviewed in (*9, 22*)]. Based on two-hybrid and co-immunoprecipitation studies, much of this modulation is proposed to result from direct protein−protein interactions between NIC and intracellular proteins. Many of these proposed interactions involve a set of ankyrin repeat sequences located near the N-terminus of NIC. Direct interactions have been suggested between these ankyrin repeats and the transcription factor Suppressor of Hairless (*23, 24*), the agonist protein Deltex (*25*), and the nuclear proteins SKIP (*26*), EMB5 (*27*), and SEL-8/LAG-3 (*28, 29*). In addition, the Notch ankyrin repeats have been proposed to self-associate to form a homotypic complex (*24*).

Ankyrin repeats are directly repeated sequences of around 33 residues (*30*). Because of the limited sequence homology among different repeats, identification of the precise beginning and ending of ankyrin repeat domains from primary

† Supported by a Basil O'Connor Starter Scholar Award from the March of Dimes (5-FY98-0719), by a Young Investigator Award from the Arnold and Mabel Beckman Foundation, and by Grant GM60001 from the National Institutes of Health.

* To whom correspondence should be addressed. TEL: (410) 516-0409. FAX: (410) 516-4118. E-mail: barrick@jhu.edu.

[1] Abbreviations: NIC, Notch intracellular domain; PCR, polymerase chain reaction; Nank1−5*, Nank1−6*, and Nank1−7*, Notch ankyrin repeat polypeptides containing five, six, and seven repeats, and with the two internal cysteines replaced with serines; Nank1−6, Notch ankyrin repeat polypeptide containing six ankyrin repeats, but containing two internal and one N-terminal cysteine; IPTG, isopropyl-*β*-D-galactopyranoside; imd, imidazole; Tris·HCl, tris(hydroxymethyl)-aminomethane hydrochloride; NTA, nitriloacetate; SDS/PAGE, sodium dodecyl sulfate−polyacrylamide gel electrophoresis; CD, circular dichroism; F_0, fluorescence in the absence of quencher; K_{SV}, Stern−Volmer constant; NATA, *N*-acetyl tryptophanamide; *s**, weight-averaged apparent sedimentation coefficient; *D**, apparent diffusion coefficient; *g*(*s**), differential sedimentation coefficient distribution function; s^0, sedimentation coefficient at infinite dilution; D^0, diffusion coefficient at infinite dilution; $s^0_{20,w}$ and $D^0_{20,w}$, sedimentation and diffusion coefficients at infinite dilution, corrected to water at 20 °C; S, Svedbergs (10^{-13} s); f_0, minimum frictional coefficient corresponding to a hydrated sphere; *a*/*b*, axial ratio of a prolate ellipsoid of revolution.

10.1021/bi011435h CCC: $20.00
Published on Web 11/07/2001

sequence can be difficult (*31*). In *Drosophila*, six ankyrin repeats have been identified from analysis of the primary sequence of Notch (*30*), although in *C. elegans*, a potential seventh ankyrin repeat has been identified in the GLP-1 Notch homologue (*31, 32*), and in human Notch, a seventh ankyrin repeat has also been identified (Steven Blacklow, personal communication).

Although the sequence variability of ankyrin repeats is high, the three-dimensional structure of several ankyrin repeat domains is quite regular (*33*). Each ankyrin repeat adopts a fold consisting of two antiparallel α-helices connected by a short loop. A second loop, which connects adjacent repeats, folds into a *β*-hairpin that is often involved in protein−protein interactions (*33*−*42*). Adjacent ankyrin repeats pack against each other to form a roughly linear array of helix pairs with an extended hydrophobic core. This overall tertiary structure differs significantly from that seen for typical globular proteins. Ankyrin repeat proteins have a regular topology, consisting of regularly spaced modules where close contacts are made by residues that are close in primary sequence, whereas typical globular proteins have irregular topologies, where close contacts are made by residues very distant in primary sequence.

The modularity of ankyrin repeat protein architecture may be reflected both in the distribution of structure along the domain and in the thermodynamics of unfolding of these proteins. First, in terms of the structural distribution across ankyrin domains, the potential for individual repeat modules to act as autonomous structural domains would allow individual repeats (or groups of modules) to be incorporated into, or removed from, preexisting domains without disrupting the overall folding pattern. Such addition and deletion of domains may result from naturally occurring mutation mechanisms (i.e., insertion, deletion, and duplication), or may be the product of protein engineering studies. The natural variation in the number of ankyrin repeats from different domains suggests some degree of structural modularity (*31*). Myotrophin, a protein containing only three ankyrin repeats, adopts a stable fold, demonstrating that small clusters of repeats can fold (*43*). Similarly, a two-repeat fragment of p16, a four ankyrin repeat tumor suppressor protein, has been engineered that folds autonomously (*44*). Second, in terms of thermodynamics of unfolding, ankyrin repeat proteins may unfold in a modular, multistate reaction controlled by short-range interactions, in contrast with the high degree of cooperativity of unfolding seen for many globular proteins.

To obtain a structural picture of the ankyrin repeat domain of the *Drosophila* Notch protein, to better define its boundaries, and to investigate the degree to which ankyrin repeat proteins display modular stability and structure distributions, we have examined solution structural and hydrodynamic properties of a variety of polypeptides derived from the ankyrin repeat region of the *Drosophila* Notch protein. Our results indicate that the Notch ankyrin polypeptides studied here adopt folded structures that are consistent, at low resolution, with known ankyrin repeat folds. We find evidence for some degree of structural modularity, in that polypeptides with different repeat number retain an overall structured conformation; however, a detailed comparison of structural parameters indicates that there are structural consequences of adding and removing individual ankyrin repeats that extend beyond the deleted repeats, suggesting that the structure of Notch ankyrin repeats is not entirely modular. In the accompanying paper (*45*), we provide evidence that there are long-range interactions that give rise to a high level of cooperative folding. Results presented here also show that the putative seventh ankyrin repeat of the *Drosophila* Notch protein is an important part of the Notch ankyrin domain. Furthermore, hydrodynamic studies presented here indicate that the Notch ankyrin repeat constructs are monomeric, indicating that, by themselves, these ankyrin repeat domains do not associate, contrary to yeast two-hybrid studies (*24, 46, 47*).

Table 1: Sequence of the Six Identified Ankyrin Repeats and the Putative Seventh Ankyrin Repeat from *Drosophila melanogaster* Notch[a]

Consensus[a]	xtx**OULHøAø**xxttxt**øø**tx**LL**txtxtxxxxxx
2° structure[b]	bb aaaaaaaaa aaaaaaaaaa bb
Repeat 1	cgl**TPL**m**IAA**vrggzq**VI**sd**LL**aqgaelnatmdk
Repeat 2	tge**T**s**LHLAA**rfarad**AA**kr**LL**dagadancqdn
Repeat 3	tgr**TPLHAAV**aadamg**VF**qi**LL**rnratnlnarmh
Repeat 4	dgt**TPL**i**LAA**rlaieg**MV**ed**L**itadadinaadn
Repeat 5	sgk**TALHWAA**avnnte**AV**ni**LL**mhhanrdaqdd
Repeat 6	kde**TPL**f**LAA**regsye**AC**ka**LL**dnfanreitdh
Repeat 7	mdrl**P**rd**VA**ser1.hhd**I**vr**LL**dehvprspqml

[a] Repeat boundaries are from Bork (*31*) except for repeat 7, which is the 32 residues immediately following the sixth repeat identified in (*31*). x = any residue, t = turn, O = Ser or Thr, U = Pro or Ala, ø = hydrophobic, z = insertion of 16 residues (gldtgediennedsta), (dot) means gap. Residues that match the consensus are in upper-case, bold. [b] Secondary structure assignments (a = α-helix, b = *β*-strand) are based on comparisons of sequences of ankyrin repeats whose structures have been determined to high resolution (*33*−*42*).

EXPERIMENTAL PROCEDURES

Subcloning and Mutagenesis. Fragments of the *Drosophila* Notch gene encoding various ankyrin repeats were amplified using the polymerase chain reaction (PCR) from a plasmid containing a cloned Notch cDNA (pMtNcDNA, a gift from Dr. Spyros Artavanis-Tsakonas). PCR primers contained *Bam*HI and *Nde*I sites on their 5′ ends to permit subsequent cloning of amplified DNA. Primers were designed to amplify DNA encoding amino acids 1901−2082 (Nank1−5), 1901−2116 (Nank1−6), and 1901−2148 (Nank1−7). PCR products were digested with *Bam*HI and *Nde*I, gel-purified on Nusieve GTG agarose (FMC), and subcloned into the pET-15b expression vector (Novagen). The resulting constructs encode N-terminal His_6-tags fused to ankyrin repeats 1−5 (Nank1−5), 1−6 (Nank1−6), and 1−7 (Nank1−7; see Table 1 for sequences). Early in the course of these studies, we replaced the cysteines with serines to improve long-term stability (Nank1−5*, Nank1−6*, and Nank1−7*, where the asterisk indicates cysteine replacement). Standard PCR mutagenesis techniques were used to substitute the cysteines in repeats 2 and 5 with serines (Table 1). The N-terminal cysteine in repeat 1 was simply omitted, as it is predicted to be in a loop region and is not likely to influence the structure or stability of the ankyrin domain. These serine-substituted polypeptides, which appear to be of similar solution structure and stability to the cysteine-containing polypeptides (see accompanying paper, *45*), are the primary subject of the work presented here.

Protein Expression and Purification. The *E. coli* strain BL21(DE3) was transformed with the pET-15b constructs

described. Five milliliters of overnight culture was used to inoculate Fernbach flasks containing 1 L of LB (*48*) containing 0.1 mg/mL ampicillin. Flasks were shaken at 37 °C until an OD_{600} of 0.7 was reached. IPTG (www.labscientific.com) was added to 1 mM, and cultures were shaken at 37 °C for 3−4 h. Bacteria were collected by centrifugation, and cell pellets were placed at −80 °C. Cell pellets were resuspended in lysis buffer consisting of 50 mM Tris·HCl, pH 8, 20 mM imidazole (imd), pH 8, 300 mM NaCl, and were disrupted using a French press (SLM Aminco). Lysed cells were centrifuged at 18 000 rpm in a JA-20 rotor for 30 min to separate the supernatant from the pellet. Nank1−7* partitioned primarily into supernatant, whereas the other constructs partitioned into the pellet. For Nank1−7*, the supernatant was loaded onto a nickel−NTA column (Qiagen) that had been equilibrated in lysis buffer, and was eluted with lysis buffer containing 250 mM imd. For the shorter constructs, pellets were solubilized in lysis buffer containing 8 M urea (resuspension buffer), and were loaded onto nickel−NTA columns that had been equilibrated in resuspension buffer. These shorter constructs were eluted with resuspension buffer containing 250 mM imd. Fractions containing Notch ankyrin repeat polypeptides were then dialyzed extensively against 50 mM Tris·HCl, pH 8, and were loaded onto a DE52 (Whatman) anion exchange column equilibrated with 50 mM Tris, pH 8. Material was eluted with a linear NaCl gradient from 0 to 1 M. Sample purity was assessed by SDS/PAGE; in some cases, faint high and low molecular weight bands were detected, and were subsequently removed by chromatography on a Sephacryl S200 gel filtration column in 25 mM Tris, 150 mM NaCl, pH 8. Purified proteins were concentrated to around 10 mg/mL, dialyzed against 25 mM Tris·HCl, 150 mM NaCl, pH 8, passed through 0.22 μm filters, and stored at −80 °C.

Concentration Determination. Protein concentrations were determined by measuring the absorbance of the aromatic side chains (one tryptophan and one tyrosine for Nank1−7* and Nank1−6*, one tryptophan for Nank1−5*) in the presence of 6 M guanidine hydrochloride, pH 6.5. Extinction coefficients were calculated as described by Edelhoch (*49*). By comparing identically prepared samples, the standard deviation in concentration determination was found to be less than 2%.

Circular Dichroism Spectroscopy. Circular dichroism (CD) spectra were collected on an Aviv 62A DS spectropolarimeter. For far-UV spectra, an 0.01 cm cell was used, with protein concentrations at roughly 100−150 μM. For near-UV spectra, a 1 cm cell was used, with protein concentrations at roughly 50 μM. For each construct, spectra were generated by averaging five wavelength scans, each obtained by signal-averaging for 1 s every 0.25 nm. To accurately determine molar ellipticity at 222 nm, a 1 cm cell was used, with protein concentrations at 2.5 μM. Samples contained 25 mM Tris·HCl, 150 mM NaCl, pH 8.0. During data acquisition, sample temperature was held at 5 °C using a thermoelectric cell holder.

Fluorescence Spectroscopy. Fluorescence emission spectra were recorded on an Aviv ATF 105 spectrofluorometer, following excitation at 295 nm. Samples were prepared as for CD (25 mM Tris·HCl, 150 mM NaCl, pH 8.0), and were diluted to roughly 5 μM prior to data acquisition. Fluorescence spectra were recorded at a sample temperature of 20 °C.

To determine the efficiency of fluorescence quenching by sodium iodide (NaI), 10 μM Notch ankyrin polypeptide in 25 mM Tris·HCl, pH 8.0, 0.5 M NaCl was titrated with a solution containing the same protein and buffer concentrations, but with 0.5 M NaI instead of NaCl. Following this procedure, ionic strength remained constant throughout the titration. Fluorescence was excited at 295 nm (2 nm bandwidth), and emission was measured at 334 nm (4 nm bandwidth). The excitation wavelength was selected to be to the low-energy side of the tryptophan absorbance transition to avoid tyrosine fluorescence. The emission wavelength was chosen as an average of the wavelength of maximum emission of Nank1−7*, Nank1−6*, and Nank1−5*, respectively.

Quenching data were analyzed using the Stern−Volmer equation:

$$\frac{F_0}{F} = 1 + K_{SV}[\mathrm{NaI}] \quad (1)$$

where F_0 is fluorescence in the absence of NaI, F is fluorescence in the presence of NaI, and K_{SV} is the Stern−Volmer constant (*50, 51*). In the absence of static quenching, the Stern−Volmer constant is equal to the product of the fluorescence lifetime and the bimolecular rate constant for collision between the chromophore (tryptophan) and the quencher (iodide), and should be related to the accessibility of the chromophore. To help interpret the Stern−Volmer constant in terms of accessibility, iodide quenching studies were performed on *N*-acetyl tryptophanamide (NATA; Sigma Chemical Co.), a model for a fully exposed tryptophanyl residue in a polypeptide. The same excitation wavelength and bandwidth were used for NATA as for the Notch Ankyrin polypeptides, but fluorescence was detected at 260 nm, the wavelength of maximum emission for NATA.

Analytical Gel Filtration Chromatography. Ankyrin repeat polypeptides were loaded onto a TosoHaas G3000PWXL 30 cm HPLC column at loading concentrations ranging from 10 to 500 μM. Samples were chromatographed in 25 mM Tris, 150 mM NaCl, pH 8, at room temperature. A molecular weight calibration curve was generated using elution times of size standards (BioRad) under the same conditions and flow rate.

Analytical Ultracentrifugation. Analytical ultracentrifugation data were collected on a Beckman XLA/XLI ultracentrifuge. Samples were dialyzed extensively against 150 mM NaCl, 25 mM Tris·HCl, pH 8.0, prior to centrifugation, and the resulting dialysate was used as a reference. Temperature was maintained at 5 °C for both velocity and sedimentation equilibrium; this low temperature slowed sedimentation during velocity runs so that a large number of scans could be collected.

Sedimentation equilibrium experiments were carried out in six-sector cells of 1.2 cm path length, or in two-sector cells of 0.3 cm path length for highly concentrated samples. Protein concentrations ranged from around 6 to 200 μM for sedimentation equilibrium runs. A range of rotor speeds (25−31 krpm) was used for sedimentation equilibrium studies, and distribution of material was monitored by absorbance at 280 nm. Equilibrium was assessed by comparing measure-

ments of concentration distributions that had been made several hours apart. When these distributions were identical within error, equilibrium was assumed. For constructs lacking cysteines, equilibrium was reached within 15−20 h. However, it was found that for samples containing cysteines, a gradual depletion of material was seen at times as long as 72 h. This depletion is likely to result from oxidative damage to the cysteines, which may result in covalently cross-linked aggregates.[2] Equilibrium data were analyzed using the program MacNonlin-PPC (*52*). Various models were fitted simultaneously to data obtained at different concentrations and rotor speeds.

Sedimentation velocity was carried out exclusively in two-sector cells at protein concentrations of 10−50 μM. Sedimentation velocity runs were centrifuged at 60 krpm, and distribution of material was monitored by absorbance at either 230 or 280 nm, depending on sample concentration. Velocity data were initially analyzed using the program DCDT (*53*−*55*) to obtain a visual representation of sedimentation and diffusional properties of the various Notch ankyrin repeat constructs. Given the relatively low *s*-values expected (and observed) for polypeptides of this size, we also analyzed the data using the program SVEDBERG to fit a single-species modified Fujita−Macosham function directly to the radial distribution data (*56, 57*). Values of *s* and *D* were extrapolated to zero protein concentration to obtain s^0 and D^0. These values were used in the Svedberg equation:

$$M = \frac{s^0 RT}{D^0(1 - \bar{\nu}\rho)} \quad (2)$$

to estimate molecular weights, where $\bar{\nu}$ is the partial specific volume of the protein (mL/g) and ρ is the solvent density. Estimates of $\bar{\nu}$ and ρ were obtained based on primary sequence (*58*) and buffer composition, respectively, using the program SEDNTERP (*59*). Values of s^0 and D^0 were subsequently corrected for the effects of low temperature, buffer, and salt composition to yield $s^0_{20,w}$ and $D^0_{20,w}$ (sedimentation and diffusion coefficients at infinite dilution in water at 20 °C) using SEDNTERP (*59*).

Axial ratios for the Notch ankyrin polypeptides were estimated with SEDNTERP (*59*). Values of $s^0_{20,w}$ were input, along with molecular weights and hydration estimates calculated from primary sequence composition, to calculate the ratio of the experimental frictional coefficient to that expected for an anhydrous sphere of the same molecular volume (f/f_{min}) and to compute the dimensions of prolate ellipsoids of revolution that are compatible with the experimental data.[3]

Bead models were constructed from ankyrin repeat structures using the program pdb2bead, written by Walter Stafford (personal communication). Hydrodynamic properties were calculated from these bead models using a version of the program HYDRO (*62, 63*) adapted to the Macintosh (Walter Stafford, personal communication).

RESULTS

Potential Notch Ankyrin Domain Boundaries. Identification of ankyrin repeats requires sequence matching to a relatively weak consensus pattern. In the *Drosophila* Notch protein (*11*), six repeats have been identified (*31, 64*). Compared to other ankyrin repeat proteins of known structure, the six identified ankyrin repeats of Notch match the ankyrin consensus sequence reasonably well (Table 1). These same ankyrin repeats are identified in a Pfam 5.5 search (*65*). In addition, weak similarity to the ankyrin repeat consensus exists in the sequence immediately C-terminal to the sixth ankyrin repeat of *Drosophila* Notch (Table 1); this C-terminal region is not identified as an ankyrin repeat in the multiple sequence alignment of Bork (*31*), or in a Pfam search. Decreased similarity to the consensus may be expected for terminal ankyrin repeats, as one of the faces of the repeat should be exposed to solvent, rather than contacting a neighboring ankyrin repeat.

To examine whether the sequence C-terminal to the sixth ankyrin repeat of *Drosophila* Notch differs from the consensus at positions predicted to be exposed to solvent, we threaded this sequence on a pair of polygons that have the rough orientation of ankyrin repeats. In an analysis of several ankyrin repeat structures, we find the packing to be best described as *i*, *i* + 3 ridges of helix 1 packing into *i*, *i* + 4 grooves of helix 2 (D. B. and K. Tripp, unpublished results). This interhelical geometry is common in globular proteins, and has been found to coincide with an interhelical angle of around 20° (*66*), consistent with the modest interhelical angle seen for ankyrin repeat structures. Such an angle prevents exact representation of the helix interface using standard helical wheels. The geometry of the helix interface can be better represented by arraying the residues of helix 1 on a triangle, and those of helix 2 on a square; residues away from the interface retain their approximate geometry in this depiction (Figure 1).

When the sequence C-terminal to the sixth ankyrin repeat of *Drosophila* Notch is arrayed as described (Figure 1), residues that match the ankyrin consensus sequence (shaded) tend to be oriented between helices, or are on the faces of the helices that would be expected to contact the sixth ankyrin repeat. In contrast, four out of five of the residues that fail to match the consensus are on the face of the first helix that would be expected to contact solvent. These observations suggest that the low sequence similarity of this C-terminal putative seventh repeat may be a result of its role as a "capping" ankyrin repeat which interacts with solvent on one face, rather than with another ankyrin repeat.

To examine the structure and stability of the ankyrin repeat region of *Drosophila* Notch, and to test whether this putative seventh repeat is incorporated into the Notch ankyrin domain, we have subcloned and expressed a Notch cDNA fragment encoding the 6 published ankyrin repeats of *Drosophila* Notch (Nank1−6*), and one that contains the 6 published repeats with the additional 32 residues of sequence C-terminal to the sixth repeat (Nank1−7*). In addition, we have

[2] Note that if intermolecular disulfide formation is responsible for this depletion, it is occurring in the presence of 1 mM DTT.

[3] Here the symbol f_{min} is used to represent the frictional coefficient of an anhydrous sphere, and f_0 is used to represent the frictional coefficient of a hydrated sphere. This nomenclature is consistent with that used by Tanford (*60*), and is similar to that used by Cantor and Schimmel (*61*). However, it differs from that used in SEDNTERP, where f_0 is used to represent the frictional coefficient of an anhydrous sphere (*59*), rather than that of a hydrated sphere. Thus, the frictional ratio calculated by SEDNTERP (designated f/f_0 in that program, and equivalent to f/f_{min} here) must be multiplied by the ratio of the unhydrated to hydrated spherical radius to obtain a shape, or Perrin factor.

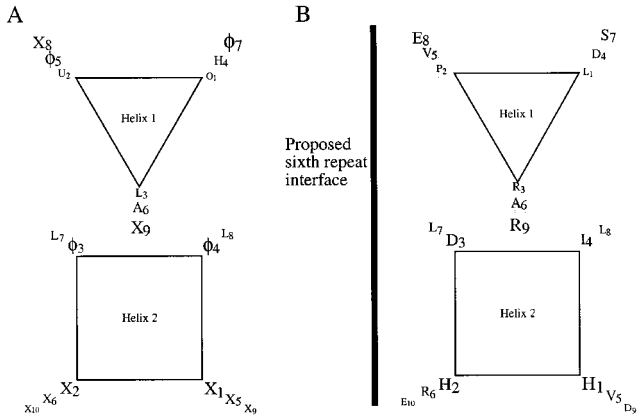

FIGURE 1: Representation of the ankyrin repeat consensus, and a possible arrangement of a seventh ankyrin repeat in *Drosophila* Notch. A. The consensus pattern for ankyrin repeats from (*31*) was placed onto two helical wheels, based on sequence analysis of several ankyrin repeat crystal structures. Because the helices within ankyrin repeats are not parallel, the orientation of the two helices is approximate. The use of a triangle and square to represent the sequences of the two ankyrin repeat helices provides a reasonable geometric representation of the interface between these two helices (see text). (B) Sequence of the putative seventh ankyrin repeat threaded onto ankyrin repeat wheels; alignment to the consensus is as in Table 1. Residues that match the consensus are shaded. The solid line indicates the interface with the sixth repeat.

expressed a construct that contains only the first through fifth repeat (Nank1−5*). This five-repeat construct has been predicted, based on yeast two-hybrid studies, to be capable of binding both to the intracellular activator protein Deltex (*25*) and to a construct containing the Notch ankyrin repeats and flanking N- and C-terminal sequences (*24*).

Far- and Near-UV Circular Dichroism Spectroscopy of the Notch Ankyrin Repeats. To examine the overall secondary structure and the degree to which the aromatic side chains (one tryptophan, one tyrosine, and four phenylalanines) are packed into fixed environments, far- and near-UV CD spectra were collected (Figure 2). The far-UV CD spectra of constructs containing repeats 1−5 (Nank1−5*), 1−6 (Nank1−6*), and 1−7 (Nank1−7*, where the "seventh repeat" is as shown in Figure 1 and Table 1) are all consistent with significant α-helical structure (Figure 2A), showing minima at 220 and 205 nm, and a maximum around 189 nm. A significant α-helical contribution to each CD spectrum is consistent with these constructs adopting the ankyrin repeat fold seen in several crystal structures (*33*−*42*). Although the far-UV CD spectra of the different Notch ankyrin repeat polypeptides have similar overall shape, there are subtle but reproducible differences in both shape and intensity. In particular, the CD spectrum of Nank1−7* has slightly deeper minima at 222 and 205.5 nm, and a higher maximum at 189 nm than that of Nank1−6*. In addition, the band at 205.5 nm is slightly red-shifted in Nank1−7* compared with Nank1−6*. Both the intensity and wavelength differences indicate that Nank1−7* has a higher α-helical content per residue than Nank1−6*. The CD spectrum of Nank1−5* is quite similar in intensity and shape to that of Nank1−6* (Figure 2A), as is the spectrum of Nank1−6, which retains the three cysteines encoded by the *Drosophila* Notch gene (not shown). To obtain a more precise quantitative estimate of the amount of α-helix in each construct, fixed-wavelength averages were measured for several independent samples of

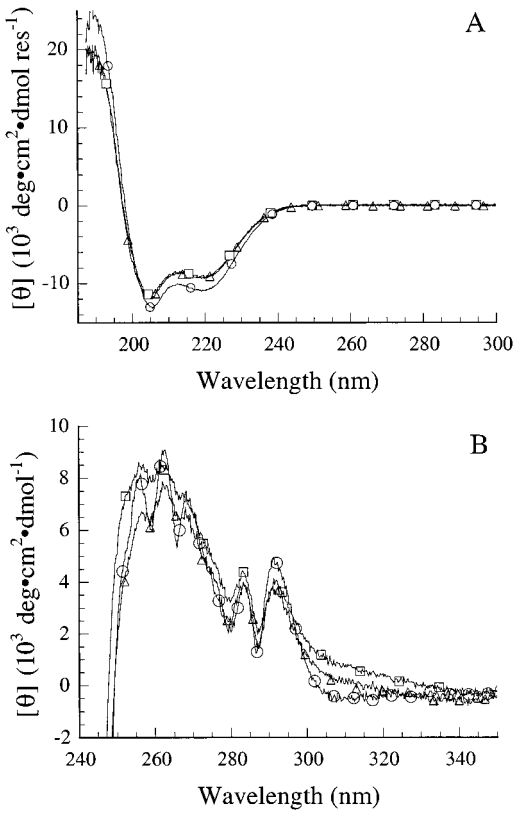

FIGURE 2: Circular dichroism spectroscopy of ankyrin repeat polypeptides from *Drosophila* Notch. (A) Far-UV spectra of Nank1−7* (○), Nank1−6* (△), and Nank1−5* (□). Samples were at 100 μM, in a cell of 0.01 cm path length. (B) Near-UV CD spectra of Nank1−7* (○), Nank1−6* (△), and Nank1−5* (□). Samples were at 50 μM, in a cell of 1 cm path length. Conditions: 25 mM Tris·HCl, 150 mM NaCl, pH 8, 5 °C.

Table 2: Circular Dichroism and Fluorescence Properties of Ankyrin Repeat Polypeptides from the *Drosophila* Notch Protein

	$[\theta]_{222}$ (deg·cm^2·dmol-res^{-1})[a]	fluorescence emission max (nm)[b]	K_{SV} (M^{-1})[c]
Nank1−7*	−9520	333.0	2.00 (2.06, 1.94)
Nank1−6*	−8070	335.5	1.39 (1.35, 1.41)
Nank1−5*	−7750	335.5	1.46 (1.49, 1.43)
NATA	nd	360.0	10.71 (10.57, 10.87)

[a] Mean molar residue ellipticity at 222 nm. Standard deviations on mean values of molar residue ellipticity are approximately 1%, and result, in large part, from error in concentration determination. [b] Emission maximum following excitation at 295 nm. [c] Stern−Volmer constant for quenching of tryptophan fluorescence with sodium iodide. K_{SV} was calculated using data at or below 0.12 M quencher.

each construct at 222 nm (a wavelength at which CD is highly sensitive to α-helical structure). Average values for each sample are presented in Table 2.

The near-UV CD spectra of these constructs show several transitions that are consistent with packing of aromatic side chains into rigid environments (Figure 2B). Nank1−7* shows five distinct peaks. The 290 and 284 nm peaks are likely to result from the single tryptophan, and the two peaks at lower wavelengths (255−265 nm) may result from two or more of the four phenylalanines. The near-UV spectra of Nank1−6* and Nank1−5* have features similar to those of the Nank1−7* spectrum, although, again, there are slight differences between the spectrum of Nank1−7* and those of

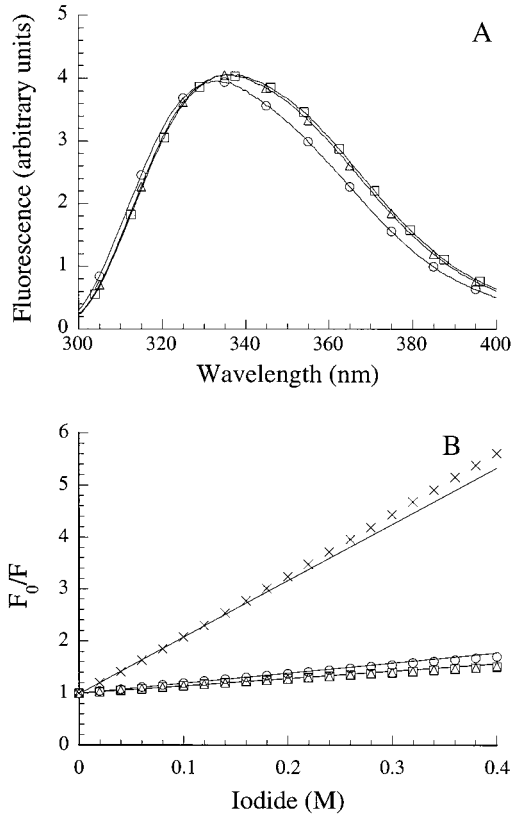

FIGURE 3: Tryptophan fluorescence spectroscopy of ankyrin repeat polypeptides from *Drosophila* Notch. (A) Emission spectra of Nank1−7* (○), Nank1−6* (△), and Nank1−5* (□), resulting from excitation at 295 nm. Sample concentrations were roughly 5 μM. Conditions: 25 mM Tris·HCl, 150 mM NaCl, pH 8, 20 °C. (B) Fluorescence quenching of Nank1−7* (○), Nank1−6* (△), Nank1−5* (□), and *N*-acetyl tryptophanamide [NATA; (×)] with sodium iodide. F_0 and F are the fluorescence signal at 330 nm (295 nm excitation), in the absence and presence of NaI, respectively. Lines result from fitting a line with unit *y*-intercept to data at or below 0.12 M sodium iodide. Conditions: 25 mM Tris·HCl, pH 8.0, total halide salt concentration is maintained at 0.5 M to provide constant ionic strength, 20 °C.

the shorter constructs. In particular, compared to the spectrum of Nank1−7*, the fine structure in the spectra of the shorter polypeptides is somewhat smoothed out. Furthermore, both of the shorter polypeptides have increased CD around 310 nm in what appears to be a shoulder. Although the peak at 268 nm might be expected to result from the single tyrosine in the sixth ankyrin repeat, this peak is present in the spectrum of Nank1−5*, which lacks this residue, indicating that this peak must have its origin in the other aromatic groups remaining in this construct [one tryptophan in repeat 5, two phenylalanines in repeats 2 and 3 (Table 1)].

Fluorescence Spectroscopy of the Notch Ankyrin Repeats. To assess the solvent polarity around the single tryptophan in the Notch ankyrin repeat polypeptides (located in repeat 5; see Table 1), the fluorescence emission spectra of Nank1−7*, Nank1−6*, and Nank1−5* were recorded. The wavelength of maximum emission for tryptophan depends on the polarity of the surroundings, shifting from around 330 nm in nonpolar environments such as protein interiors to 350−360 nm in water. For Nank1−7*, the wavelength of maximum emission in the tryptophan fluorescence spectrum is 333 nm (Figure 3A), indicating that the environment surrounding the tryptophan is significantly nonpolar. For the shorter Notch ankyrin constructs, there is a small shift to longer wavelength, with a maximum emission wavelength of 335.5 nm for both Nank1−6* and Nank1−5*. These results indicate a slight perturbation around the repeat 5 tryptophan of Nank1−6* and Nank1−5*.

To probe the accessibility of the tryptophan in repeat 5 to solvent, fluorescence quenching studies were performed on Nank1−7*, Nank1−6*, and Nank1−5*. Iodide anion is a strong collisional fluorescence quencher of exposed tryptophans, especially in polar environments. Addition of sodium iodide (NaI) to the Notch ankyrin repeat constructs decreases fluorescence (Figure 3B; in the Stern−Volmer representation, inverse fluorescence is plotted as a function of quencher concentration, leading to a rise in the independent variable with increased quencher). A much larger degree of quenching is seen for NATA in aqueous buffer, resulting in a steeper slope in the Stern−Volmer plot (Figure 3B). NATA, a derivative of tryptophan, should be completely accessible to the quenching agent, and thus should provide an upper limit for quenching.

Slight deviations from linearity in the Stern−Volmer representation are seen for the Notch ankyrin constructs as well as for NATA. For the Notch ankyrin repeats, a slight decrease in slope is seen at high NaI concentrations. Similar downward curvature has been seen in acrylamide quenching studies of liver alcohol dehydrogenase (*50*, *67*), and was attributed to multiple fluorophores with different properties. Although the Notch ankyrin constructs studied here contain a single tryptophan, residual tyrosine fluorescence may be contributing to this downward curvature, although at the excitation wavelength used (295 nm), very little tyrosine excitation should occur. Another possible explanation for the downward curvature is that the quencher may be inefficient: the quencher−fluorophore encounter complex may decay by dissociation and/or fluorescence, rather than thermal deexcitation. For NATA, the slight upward curvature at high NaI concentrations may result from static quenching.

Because of the slight nonlinearity in the Stern−Volmer plots, we have used only fluorescence data at low quencher concentrations (at or below 0.12 M) to determine Stern−Volmer constants (fitted lines, Figure 3B; Table 2). Using this limited portion of the data, fitted Stern−Volmer constants for Nank1−6* and Nank1−5* are nearly identical (1.39, 1.46 M^{-1}, respectively), whereas that for Nank1−7* is slightly increased (2.0 M^{-1}). These Stern−Volmer constants are significantly less than that measured for NATA (10.7 M^{-1}), indicating that for all Notch ankyrin constructs, the single tryptophan is shielded from quencher, consistent with the nonpolar environment inferred from tryptophan fluorescence emission above. Also consistent with the fluorescence emission data, the quenching studies indicate that for Nank1−6* and Nank1−5*, the tryptophan is in a similar environment, and that this environment differs somewhat from that of Nank1−7*. However, the modest increase in accessibility of the tryptophan in Nank1−7* to iodide is somewhat surprising, given the slight blue-shift in its fluorescence emission spectrum, relative to those of Nank1−6* and Nank1−5*.

Gel Filtration Chromatography of the Notch Ankyrin Repeats. The oligomeric state of the Notch ankyrin repeat

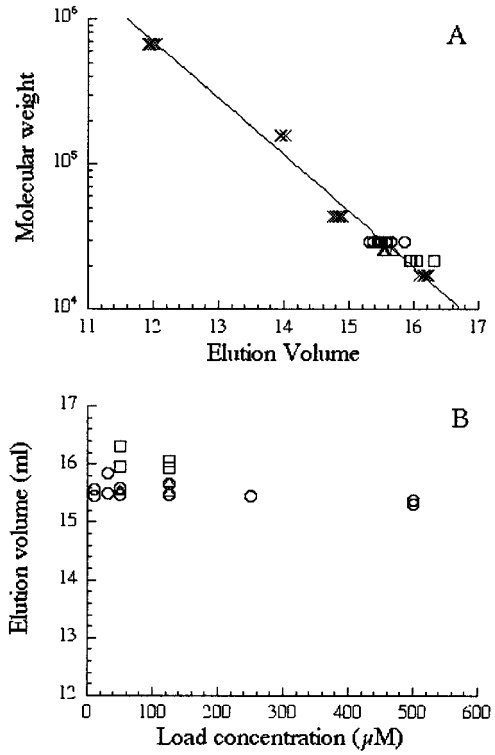

FIGURE 4: Gel filtration chromatography of ankyrin repeat polypeptides from *Drosophila* Notch. (A) Elution volume versus predicted molecular weight. Symbols indicate molecular weight standards (×), Nank1−7* (○), Nank1−6* (△), and Nank1−5* (□). Multiple symbols show the result of independent chromatograms. Molecular weights for standards are thyroglobulin, 670 000; γ-globulin, 158 000; ovalbumin, 44 000; and myoglobin, 17 000. For the ankyrin repeat polypeptides, ordinate values are the calculated monomer molecular weights. (B) Dependence of elution volume on the loading concentration of ankyrin repeat proteins. Symbols are as in (A). Conditions: 25 mM Tris·HCl, 150 mM NaCl, pH 8, room temperature.

polypeptides was assessed by gel filtration chromatography. Comparison of elution times of the ankyrin repeat polypeptides with elution times of size standards is consistent with a largely monomeric state (Figure 4A, Table 3). Although gel filtration chromatography is not likely to detect low concentrations of associated species, the elution times are independent of loading concentration over a 50-fold range (10−500 μM, Figure 4B), demonstrating that at the concentrations used for CD spectroscopy (2.5−150 μM), the Notch ankyrin repeat polypeptides studied here are predominantly monomeric.

Sedimentation Equilibrium of the Notch Ankyrin Repeats. To further examine the oligomeric state of the Notch ankyrin repeat constructs, analytical ultracentrifugation experiments were performed in equilibrium mode. Equilibrium distributions of Nank1−7* at different concentrations and rotor speeds are shown in Figure 5. These data can be well-fitted to a single-component model using the program MacNonlin-PPC (*52*) (solid lines, Figure 5), resulting in a random distribution of residuals (Figure 5, top). Similar results were obtained for Nank1−6* and Nank1−5* (not shown). If the Notch ankyrin polypeptides were significantly populating multiple oligomeric states, deviation from the single-component model would be expected. Thus, the Notch ankyrin polypeptides seem to exist as a single stoichiometric species over the concentration range examined (6−200 μM). Using values of the partial molar volume based on amino acid sequence (*58*, *59*), molecular weights of 30 200, 28 400, and 24 500 were obtained for Nank1−7*, Nank1−6*, and Nank1−5*, respectively. These values are close to the predicted monomer molecular weight from primary sequence (Table 3), with deviations of around 4% for Nank1−7*, and around 14% for Nank1−6* and Nank1−5*. Although deviations are toward higher molecular weight for all three polypeptides, the molecular weights determined by sedimentation equilibrium are all much closer to monomeric values than to dimeric values.

Sedimentation Velocity of the Notch Ankyrin Repeats. To further assess the oligomeric state of the Notch ankyrin repeat polypeptides, and to obtain information about their hydrodynamic shape, we have performed sedimentation velocity experiments on the Notch ankyrin repeat polypeptides. Sets of sedimentation velocity curves were analyzed using the program DCDT (*53*, *54*) to provide an intuitive representation of the sedimentation properties of the sample. DCDT produces a sedimentation coefficient probability distribution, represented by the differential probability function $g(s^*)$. Such distributions, or $g(s^*)$ plots, are shown for Nank1−7*, Nank1−6*, and Nank1−5* in Figure 6A. For a single sedimenting species, the plot has a Gaussian shape centered at the weight-average apparent sedimentation coefficient (s^*), and a width proportional to the translational diffusion coefficient for the species (*53*−*55*). Single-component fits are shown as solid lines in Figure 6A. As with the equilibrium data, a single-component fit provides an adequate description of the data, indicating a single stoichiometric species. Comparison of the normalized $g(s^*)$ plots of the Notch ankyrin polypeptides indicates a progressive decrease in s^* as repeats are removed, although the decrease in s^* is largest going from Nank1−7* to Nank1−6*, with only a modest decrease going from Nank1−6* to Nank1−5*. In contrast, the largest increase in the apparent translational diffusion coefficient, estimated by the width of the $g(s^*)$ plot, occurs in going from Nank1−6* to Nank1−5* (Figure 6A).

To more accurately quantify sedimentation and diffusion coefficients, the program SVEDBERG (*56*, *57*) was used to analyze s^* and D^* values for Nank1−7*, Nank1−6*, and Nank1−5* at different concentrations.[4] Values of s^* and D^* were plotted as a function of loading concentration to examine the effect of concentration on s^*, and to estimate the values of s and D at infinite dilution (s^0, D^0). Values of s^* are essentially independent of concentration over the range examined, from 0.25 to 1 mg/mL (roughly 10−40 μM, Figure 6B), again consistent with the idea that only a single oligomeric state is populated over this concentration range. Values of D^* show a very modest increase with concentration; although this trend is not expected, it is likely to be within error of the values of D^*. Values of s and D at infinite dilution (s^0 and D^0) were estimated from intercepts of linear fits of s^* and D^* versus concentration (Figure 6B, Table 3).

[4] The program SVEDBERG was used because it provides a more reliable determination of numerically small s values (as are expected here) than DCDT, and because SVEDBERG permits analysis of scans evenly distributed throughout the run (*57*), allowing multiple cells to be analyzed simultaneously using absorbance optics.

Table 3: Hydrodynamic Properties of Ankyrin Repeat Polypeptides from the *Drosophila* Notch Protein[a]

	predicted from sequence	gel filtration	sedimentation equilibrium	sedimentation velocity				
	M	M^b	M^c	$s^0_{20,w}{}^d$	$D^0_{20,w}{}^d$	M^e	$f/f_0{}^f$	a/b^g
Nank1−7*	28830	30000	30200	2.41	0.74	29232	1.24	4.9
Nank1−6*	24929	28000	28400	2.11	0.76	25240	1.29	5.7
Nank1−5*	21244	18000	24500	2.04	0.90	20644	1.20	4.3

[a] All measurements made in 150 mM NaCl, 25 mM Tris·HCl, pH 8.0. [b] Average values of molecular weight estimated from loading concentrations ranging from 10 to 500 μM; standard deviations of the mean are 300, 450, and 700 for Nank1−7*, Nank1−6*, and Nank1−5*, respectively. [c] Determined from multiple protein concentrations and rotor speeds as described under Experimental Procedures. [d] Values of $s^0_{20,w}$ (in Svedbergs, $\times 10^{-13}$ s) and $D^0_{20,w}$ ($\times 10^{-6}$ cm^2·s^{-1}) were obtained by extrapolating values of s* and D* to zero concentration (Figure 6B), and then correcting for the effects of temperature, buffer, and salt concentration. [e] Calculated from the Svedberg equation using partial specific volumes based on the amino acid composition of each of the three polypeptides (*58*, *59*). [f] The ratio of the experimentally determined frictional coefficient to that expected for an equivalently hydrated sphere of the same mass and volume. [g] Axial ratios calculated using the program SEDNTERP (*59*, *61*).

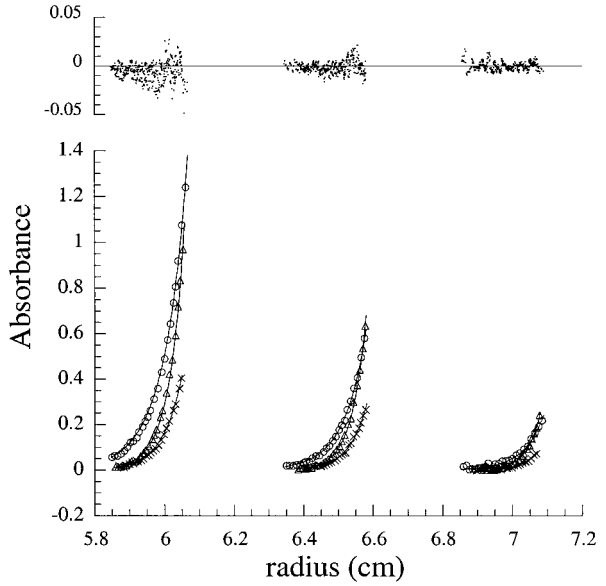

FIGURE 5: Equilibrium ultracentrifugation of Nank1−7*. Absorbance at 235 nm versus radial position at three different concentrations and rotor speeds. Loading concentrations were 58 (inner sector), 19 (middle sector), and 6 μM (outer sector). Symbols indicate speeds of 25 krpm (○), 28 krpm (×), and 31 krpm (△). Solid lines are the results of simultaneous fitting of an ideal single-species model to the data. Combined residuals for all 3 speeds and concentrations are shown above (1096 points total). Note that the scale for the plot of residuals is around 5 times that of the data. Conditions: 25 mM Tris·HCl, 150 mM NaCl, pH 8, 5 °C.

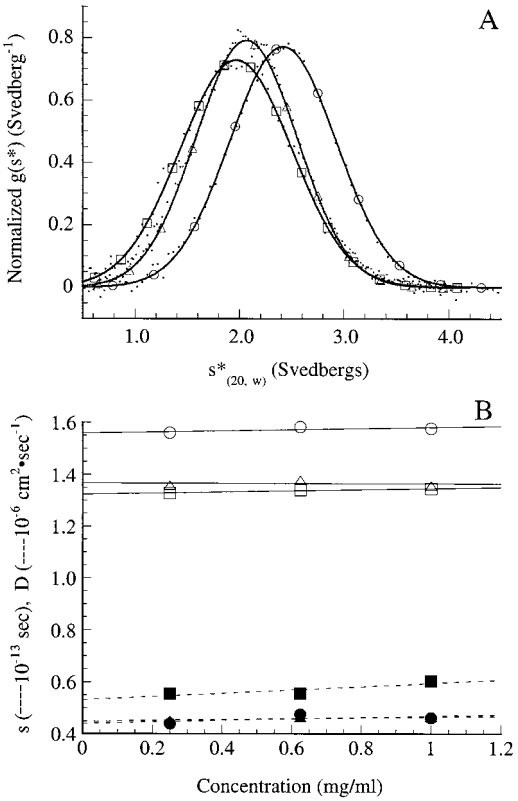

FIGURE 6: Sedimentation velocity of Notch ankyrin repeat polypeptides. (A) Normalized $g(s^*)$ representation of sedimentation coefficients for Nank1−7* (○), Nank1−6* (△), and Nank1−5* (□). The ordinate indicates the fraction of total material sedimenting at a given s-value. To obtain normalized $g(s^*)$ plots, the distribution of data was numerically integrated for each polypeptide and was divided into the original $g(s^*)$ values. This normalization corrects for differences in concentration and step-size, giving each distribution unit area. Smooth lines represent single-component fits to the data. (B) Sedimentation and diffusion coefficients (open and filled symbols, determined using SVEDBERG) as a function of loading concentration. Estimates of s^0 and D^0 are obtained as intercepts defined by linear fits to the data (solid and dashed lines, respectively).

These values were then combined with partial molar volume estimates to evaluate molecular weights using the Svedberg equation (eq 2). Estimated molecular weights are in close agreement with monomer molecular weights predicted from primary sequence, deviating by 0.9, 0.7, and 3.0% for Nank1−7*, Nank1−6*, and Nank1−5*, respectively (Table 3).

To evaluate the frictional properties of the Notch ankyrin repeat polypeptides, values for s^0 and D^0 were extrapolated to 20 °C and to pure water as solvent ($s^0_{20,w}$ and $D^0_{20,w}$, Table 3). As seen qualitatively in the $g(s^*)$ plots of Figure 6A, $s^0_{20,w}$ decreases substantially as a result of removing the seventh ankyrin repeat (from 2.41 to 2.11 S) whereas further truncation that results from removing the sixth repeat decreases $s^0_{20,w}$ only slightly (from 2.11 to 2.04 S). In contrast, $D^0_{20,w}$ showed only a modest increase as a result of removing the seventh ankyrin repeat (from 0.75×10^{-6} to 0.76×10^{-6} cm^2·s^{-1}), but increased substantially as a result of further truncation (from 0.76×10^{-6} to 0.90×10^{-6} cm^2·s^{-1}). These abrupt changes indicate that the frictional properties of Nank1−7*, Nank1−6*, and Nank1−5* differ substantially from one another, and suggest that the molecular dimensions of these polypeptides do not simply vary in proportion to the number of repeats.

One way to examine the frictional properties that takes into account the changes in the molecular weight of Notch polypeptides with different numbers of ankyrin repeats is to

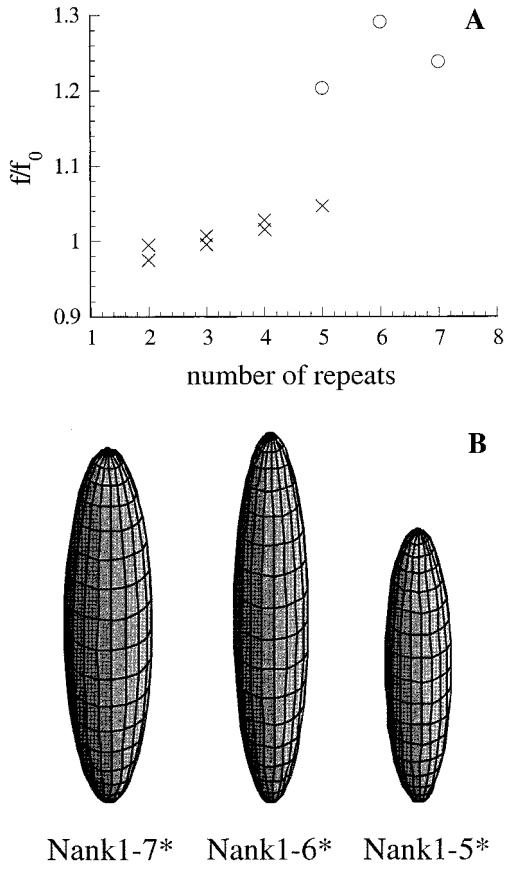

FIGURE 7: Experimental and calculated hydrodynamic properties of Notch ankyrin repeat polypeptides. (A) Comparison of experimentally determined shape factors (f/f_0) for Notch ankyrin repeat polypeptides (○) with values calculated from bead models built from ankyrin repeat proteins of known structure (×). Bead models were constructed from the coordinates of the five-repeat protein p18INK4c [pdb code 1IHB (*42*)] and from N- and C-terminal fragments containing fewer repeats. These bead models consist of spheres of identical radius centered on each α-carbon; summed sphere volumes equal the molecular volume estimated from primary sequence. Sedimentation and diffusion coefficients were calculated for each bead model using the program HYDRO (*62, 63*), and were converted to shape factors using the program SEDNTERP (*59*). (B) Prolate ellipsoids of revolution with frictional properties matching experimentally determined values for the Notch ankyrin constructs. These ellipsoids are depicted using MATHEMATICA (*80*) to plot surfaces defined by the parametric equations $x = b\cos(u)\cos(t)$, $y = b\sin(t)\cos(u)$, $z = a\sin(u)$, where a and b are the major and minor semiaxes of the ellipsoids, and the parameters u and t vary over the range $\{0 \leq t \leq 2\pi\}$, $\{-\pi/2 \leq u \leq \pi/2\}$. From the hydrodynamic analysis, values of a and b are 7.2, 7.55, and 5.6 nm, and 1.35, 1.2, and 1.1 nm for Nank1−7*, Nank1−6*, and Nank1−5*, respectively.

compare experimental frictional coefficients with those calculated assuming an equivalently hydrated sphere (f_0) of the same molecular volume. If the Notch ankyrin polypeptides adopt a hydrated spherical shape, the ratios of the observed and hypothetical minimum frictional coefficients [f/f_0, also known as a "shape", or "Perrin" factors (*61*)] should be equal to 1, and should be insensitive to molecular volume, i.e., the number of ankyrin repeats in the Notch constructs. If instead an elongated shape is adopted (as is expected for a folded ankyrin domain), f/f_0 should be larger than 1, and should decrease steadily as repeats are removed and axial asymmetry is decreased (Figure 7A, ×'s). However, the Notch ankyrin repeat constructs studied here show neither of these behaviors (Figure 7A, Table 3). Instead, f/f_0 is larger for Nank1−6* than for Nank1−7*, indicating that removal of the putative seventh ankyrin repeat increases the frictional coefficient of the remaining polypeptide relative to the corresponding hydrated sphere. This effect reverses for Nank1−5*, for which f/f_0 is less than those of Nank1−6* and Nank1−7*.

Given the elongated structure expected for an ankyrin domain, it seems reasonable to interpret shape information for the Notch ankyrin repeats using prolate ellipsoids of revolution as structural models. By assuming a hydration value based on amino acid composition (*59, 68*), the experimentally determined frictional ratios can be used to determine the length and ratio of the major and minor semiaxes of prolate ellipsoids that would have the same frictional properties as determined for the Notch ankyrin polypeptides. Clearly, these ellipsoid shapes are not unambiguously determined by the data; rather, they provide a general picture that is consistent with experimentally determined frictional properties. The three prolate ellipsoids with frictional properties corresponding to Nank1−7*, Nank1−6*, and Nank1−5* are shown in Figure 7B. To match the experimentally determined hydrodynamic data, the prolate ellipsoid that is frictionally equivalent to Nank1−6* would have to be more elongated than the ellipsoid matching the frictional properties of Nank1−7* (Figure 7B, Table 3). The ellipsoid that is frictionally equivalent to Nank1−5* would be less elongated than either of the two longer polypeptides. Whereas the decrease in axial ratio for Nank1−5* is expected from considerations of the effects of shortening an ankyrin repeat domain, the increase for Nank1−6* compared to Nank1−7* demands a more elaborate hydrodynamic model than simple prolate ellipsoids can provide, such as one involving partial unfolding.

DISCUSSION

The ankyrin repeat region of the Notch receptor is critical for signaling. Molecular biological techniques, such as the yeast two-hybrid assay, have identified a number of putative protein−protein interactions that involve the ankyrin repeat region of Notch, including direct homotypic association (*23−25, 27−29*). Structural information on the ankyrin region of the Notch polypeptide will be essential for developing a detailed understanding of the molecular mechanisms behind Notch signaling. The results presented in this paper provide insight into the overall structure of the Notch ankyrin repeat region, help to delineate the boundaries of the ankyrin domain, and ascertain the oligomeric state of this domain in solution. The results presented in this and the accompanying paper (*45*) also provide information on the degree to which the modular architecture of ankyrin repeat proteins results in modular structure and stability.

Overall Structural Similarities among Notch Ankyrin Repeat Polypeptides. Based on the spectroscopic and hydrodynamic measurements made here, the Notch ankyrin repeat region appears to be folded into a monomeric but somewhat elongated structure with significant α-helical secondary structure and fixed tertiary interactions. Far-UV CD spectroscopy indicates a significant amount of α-helical structure (Figure 2, Table 2). Although the shapes of the CD spectra are consistent with significant helix content, the

magnitude of the observed ellipticity appears to be somewhat low, considering the crystal structures of several ankyrin repeat proteins (*33*−*42*), in which over 50% of each repeat is α-helical. One possible explanation for the low observed ellipticity is that all of the helices are expected to be short, either 9 or 10 residues in length. The CD of α-helices is both predicted and observed to be length-dependent, with shorter helices producing less ellipticity per residue than longer ones (*69*−*71*). Another possible explanation for the low observed ellipticity is that one or more of the repeats on the N-terminus is disordered. The studies here examine participation in the ankyrin domain of repeats on the C-terminus, but not the N-terminus. Although the ellipticity of the Notch ankyrin polypeptides is lower than expected based on crystal structures of other ankyrin repeat proteins, the CD spectra are consistent both in shape and in magnitude with CD spectra of other ankyrin repeat domains (*44*, *72*−*75*), including p16, where high-resolution structural data indicate that each ankyrin repeat adopts an ordered ankyrin fold (*41*, *76*).

Near-UV CD shows several bands from 250 to 300 nm (Figure 2B). These bands are likely to result from exciton coupling of aromatic side chains, which requires these side chains to occupy fixed orientations with respect to each other (*61*, *77*). The observation that Nank1−5* (which is missing one tyrosine and two phenylalanine residues that are present in repeat 6 of the longer constructs) retains a near-UV CD spectrum similar to the longer polypeptides suggests that at least some part of the near-UV CD spectrum (especially from 250 to ∼270 nm) must result from the phenylalanine residues in repeats 2 and 3. Thus, rigid tertiary structure in the Notch ankyrin domain appears to include repeats 2 and 3.

Unlike near-UV CD, which in principle probes the rigidity of all of the aromatic side chains (tryptophan, phenylalanine, and tyrosine) in the Notch ankyrin repeats, fluorescence spectroscopy (Figure 3) reports on the accessibility and polarity of the environment surrounding the single tryptophan in repeat 5 (Table 1). Based on the wavelengths of maximum emission, the environment surrounding the tryptophan in repeat 5 appears to be rather nonpolar in all constructs studied. Based on the fluorescence quenching, this tryptophan appears to be sequestered from solvent. These findings are particularly significant for Nank1−5*, since removal of the sixth and putative seventh repeats should expose part of the fifth repeat to solvent. In the sequence alignment in Table 1, the tryptophan in repeat 5 occupies the ϕ5 position, which would pack against the N-terminal adjacent repeat (repeat 4). The observation that the tryptophan in Nank1−5* remains in a nonpolar environment is consistent with this model. These spectroscopic features indicate that all three Notch ankyrin polypeptides studied here contain a common region of well-folded structure extending from repeat 2 through repeat 5, and at low resolution, this common structure is consistent with known structures of other ankyrin repeat proteins.

Based on sedimentation velocity studies, the ankyrin repeat polypeptides have high frictional coefficients, suggesting elongated structures. The shape factors determined here for the Notch ankyrin repeats result in calculated axial ratios (*a*/*b*) of around 5 (Table 3), assuming a prolate ellipsoidal shape. Although axial distortion is qualitatively consistent with known ankyrin repeat structures, the magnitude of this distortion is larger than expected based on the known structures of ankyrin domains. To illustrate this, shape factors were calculated from bead models (*62*, *63*) constructed from known ankyrin repeat structures. These calculated shape factors increase with increasing repeat number, consistent with increased axial asymmetry. However, for the longest structure analyzed (five repeats), the shape factor only increases to a value of 1.05, significantly lower than that determined for the five-repeat Notch polypeptide (Figure 7A). One explanation for the high apparent axial ratios for the Notch ankyrin polypeptides is that a portion of each of the Notch ankyrin polypeptides is unfolded, and is thus increasing the frictional properties of the polypeptide; this unfolded region likely includes the N-terminal His-tag present on each polypeptide, but may also extend into the N-terminal repeat of each construct. We note that shape factors similar those measured for the Notch constructs were obtained in hydrodynamic studies of a series of six-repeat proteolytic fragments of ankyrin, the cytoskeletal protein from which the repeat name derives (values of f/f_0 range from 1.2 to 1.3) (*74*). Although the numerical values of the shape factors of the ankyrin fragments were interpreted as indicative of spherical shape by the authors (*74*), we interpret their shape factors as an indication of high axial distortion for ankyrin fragments.

Structural Differences among Notch Polypeptides with Different Repeat Numbers. Despite the overall similarities in the secondary and tertiary structure of the seven-, six-, and five-repeat Notch ankyrin polypeptides, there are small but reproducible spectroscopic and hydrodynamic differences between Nank1−7* and the shorter constructs, indicating structural differences. Slightly weaker (less negative) molar residue ellipticity values in the far-UV CD spectra of Nank1−6* and Nank1−5* (Figure 2A, Table 1) indicate that the shorter constructs have lower percentages of α-helical structure. As these ellipticity values are normalized to the number of residues in each polypeptide, this is not simply a result of losing helices of the putative seventh ankyrin repeat by deletion; rather, it suggests that some of the α-helical structure present in repeats 1−6 of the full-length construct is lost upon removal of the putative seventh repeat.

The near-UV CD spectra also indicate minor structural changes for Nank1−6* and Nank1−5*. Although the spectra of all constructs have the same number of resolved peaks, and these peaks appear at the same wavelengths, the peaks are considerably better resolved in the spectrum of Nank1−7* than in the spectra of the two shorter constructs. Because the sixth ankyrin repeat contains one tyrosine and two phenylalanines, changes in the near-UV CD spectrum of Nank1−5* are not entirely unexpected. However, for Nank1−6* these residues are retained, yet the near-UV CD spectrum shows the same decreased resolution as for Nank1−5*. Thus, the changes in the near-UV CD spectra of the five and six-repeat polypeptides must originate either from minor structural changes of the aromatic chromophores in the first five repeats, or from disruption of the sixth repeat in Nank1−6* as a result of deleting the putative seventh repeat. This second interpretation is consistent with the loss of α-helical content seen for Nank1−6*.

Like the far- and near-UV CD data, the tryptophan fluorescence data also indicate minor structural changes for the five- and six-repeat constructs, compared to the seven-repeat construct. There is a small but reproducible red-shift (2−3 nm) in the emission maxima of Nank1−5* and Nank1−6*, compared to that of Nank1−7* (Figure 3A, Table 2), indicating a slight increase in the polarity of the environment surrounding the tryptophan in repeat 5. It is possible that this slight shift is caused by a minor structural rearrangement resulting from loss of structure in the adjacent (sixth) repeat. Identical changes in the emission maximum of the six- and five-repeat polypeptides would again be expected if deletion of the putative seventh repeat disorders the sixth repeat in the Nank1−6* polypeptide, so that further truncation to Nank1−5* results in no further loss of ordered structure. This structural model is also consistent with the observation that quenching of tryptophan fluorescence in Nank1−6* and Nank1−5* is perturbed to the same degree compared to Nank1−7* (Figure 3B, Table 2). However, the slight decrease in quenching of the shorter polypeptides (indicative of decreased accessibility) is somewhat surprising, given the increase in the wavelength maximum of fluorescence of the shorter polypeptides (indicative of increased polarity), as these two quantities typically show a positive correlation (*51*).

Sedimentation velocity data are also consistent with partial unfolding of the sixth repeat in the absence of the putative seventh repeat. Assuming an elongated, prolate structure, deletion of terminal repeats should bring about a monotonic decrease in shape factors and, as a result, calculated axial ratios. Indeed, this trend is seen in shape factors calculated from hydrodynamic modeling of ankyrin repeat structures (Figure 7A). While a decrease in shape factor (and thus axial ratio) is seen in a comparison of Nank1−7* with Nank1−5*, Nank1−6* has a larger shape factor (and thus a larger calculated axial ratio) than Nank1−7* (Table 3, Figure 7A). Thus, the variation of measured Notch ankyrin shape factors (and computed axial ratios) with repeat number is inconsistent with a simple model in which deletion of ankyrin repeats simply produces a shorter array of folded repeats (Figure 7), but is consistent with the a model in which the sixth repeat is unfolded in the absence of the seventh repeat (i.e., Nank1−6*). Unfolding of the sixth repeat in the absence of the seventh repeat would increase the frictional coefficient of Nank1−6* compared with Nank1−7*, and deletion of this unfolded sixth repeat would significantly decrease the frictional coefficient of Nank1−5*, as is observed experimentally.

Oligomeric State of Notch Ankyrin Repeat Polypeptides. Since the ankyrin domain of the Notch receptor is thought to interact directly with several other proteins, determining the oligomeric state of the Notch ankyrin repeat domain is an important first step in quantifying the stoichiometries and affinities of the various noncovalent complexes that regulate Notch signaling. In particular, determination of the oligomeric state of the Notch ankyrin polypeptides should provide insight into a proposed homotypic interaction between the ankyrin repeats of *Drosophila* Notch and a construct composed of the entire Notch intracellular domain (*24*), and into interactions identified between similar ankyrin repeat constructs from the worm glp-1 Notch homologue (*46*). The constructs we are using to examine the oligomeric state appear to be appropriate for interaction studies, as they seem well-structured based both on the spectroscopic data above and on the thermodynamic data in the accompanying paper (*45*).

All of the hydrodynamic methods we have used to determine the oligomeric state of the *Drosophila* Notch ankyrin repeats indicate that the three constructs are monomeric over a broad range of concentrations (Figures 4−6, Table 3). For gel filtration chromatography, loading concentrations ranged from 10 to 120 μM (and as high as 500 μM for Nank1−7*). For velocity sedimentation, loading concentrations ranged from approximately 7 to 50 μM, and for sedimentation equilibrium, loading concentrations ranged from approximately 20 to 200 μM. These findings are consistent with the observation that unfolding transitions of these Notch ankyrin polypeptides are insensitive to protein concentration [see accompanying paper (*45*)]. The observation that all three constructs studied here are monomeric is important for interpreting the conformational differences between the seven-repeat polypeptide and the six- and five-repeat polypeptides; demonstrating that these differences are not a result of dissociation of a complex in response to truncation, but rather are a change in monomeric solution structure. The fact that these well-folded *Drosophila* Notch ankyrin domains remain monomeric at concentrations greater than 0.25 mM indicates either that the homotypic interaction detected by yeast two-hybrid methods is quite weak on its own ($K_d > \sim 1$ mM) or that the interaction requires components outside the ankyrin domain. Specifically, the homotypic interaction detected in the two-hybrid studies may involve a stabilizing interaction between the ankyrin repeat domain and a separate region of the Notch intracellular domain, since the two-hybrid experiment tested for interaction between the first six ankyrin repeats and the entire intracellular domain (*24*).

Importance of the Putative Seventh Repeat for Structural Integrity. Although sequence identity among ankyrin repeats is relatively low (*30*, *31*), the fact that multiple copies of ankyrin sequences are found in tandem makes identification of ankyrin domains relatively straightforward. However, identification of the ends of an ankyrin domain presents a challenge both because terminal repeats may deviate from the consensus sequence as a result of increased solvent exposure, and because adjoining sequences may fortuitously match the relatively weak consensus. For the *Drosophila* Notch ankyrin repeats, the average pairwise identity of repeats 1−6, as aligned in Table 1, is 31.5%, whereas the average pairwise identity of the putative repeat 7 with repeats 1−6 is only 17%. As a result of this low identity, the putative seventh repeat sequence was not identified as an ankyrin repeat in an extensive search for ankyrin sequences (*31*).

The spectroscopic and hydrodynamic studies demonstrate that the C-terminal putative ankyrin repeat sequence is an important part of the *Drosophila* ankyrin domain, despite the poor match of this sequence to the ankyrin consensus. Not only does it appear that the putative seventh repeat is incorporated into the ankyrin fold, it appears that this region facilitates further structuring of at least some of the six previously identified repeats. In particular, the spectroscopic and sedimentation velocity studies presented here are consistent with a role for the putative seventh repeat in inducing structure in the sixth repeat, and without the seventh repeat,

the sixth repeat appears to unfold despite the good match of the sixth repeat to the ankyrin consensus. These conclusions are strongly supported by the results in the accompanying paper (*45*), which demonstrate that the putative seventh ankyrin repeat greatly stabilizes the entire ankyrin domain, and increases thermodynamic quantities that are sensitive to the number of residues participating in a folding transition. Based on the data presented in this and the accompanying paper (*45*), it seems quite likely that the C-terminal sequence exerts its ordering, stabilizing effect on the ankyrin domain by adopting an ankyrin fold and packing against the sixth repeat via a typical ankyrin−ankyrin interaction. However, it is possible that although this C-terminal sequence stabilizes the Notch ankyrin domain through direct interactions, it adopts a different fold. This mode of capping of repeat proteins has been seen in the leucine-rich repeats of dynein motor domain associated light chain (*78*), in the TPR repeats of Sec17 (*79*), and in the ankyrin repeats of Swi6 (*35*). Determination of the precise structural means by which this C-terminal sequence stabilizes the Notch ankyrin domain will require high-resolution structural information.

Although the putative seventh ankyrin repeat identified here for the *Drosophila* Notch protein has escaped sequence analysis, a seventh ankyrin repeat sequence has been identified in a human Notch homologue (Stephen Blacklow, personal communication). In addition, seven potential ankyrin repeats have been reported in the Notch receptors encoded by the *glp*-1 and *lin*-12 genes of *Caeonrhabditis elegans* (*31*, *32*). Interestingly, the seven *Glp*-1 ankyrin repeats identified by Roehl et al. (*32*) are shifted by one repeat relative to those identified by Bork (*31*), raising the possibility that in the *Glp*-1 Notch homologue, there may be eight repeats in the ankyrin domain. Experiments such as those described here and in the accompanying paper (*45*) will should help resolve the number and locations of the ankyrin repeats in the Notch homologues of *C. elegans*, as well as on the N-terminal end of the *Drosophila* Notch ankyrin domain.

ACKNOWLEDGMENT

We thank Spyros Artavanis-Tsakonas and Kenji Matsuno for providing us with a Notch cDNA clone. We are grateful to Steven Blacklow for informing us of a potential seventh ankyrin repeat in Notch. We thank Karen Fleming and Mike Rodgers for advice and assistance in collecting and analyzing analytical ultracentrifugation data. We thank Walter Stafford for sharing unpublished software for structure-based hydrodynamic modeling. We thank Debbie Andrew and Karen Fleming for critically reading the manuscript.

REFERENCES

1. Artavanis-Tsakonas, S., Rand, M. D., and Lake, R. J. (1999) *Science 284*, 770−776.
2. Bray, S. (1998) *Cell 93*, 499−503.
3. Kimble, J., and Simpson, P. (1997) *Annu. Rev. Cell Dev. Biol. 13*, 333−361.
4. Kopan, R., and Cagan, R. (1997) *Trends Genet. 13*, 465−467.
5. Muskavitch, M. A. (1994) *Dev. Biol. 166*, 415−430.
6. Posakony, J. W. (1994) *Cell 76*, 415−418.
7. Artavanis-Tsakonas, S. (1997) *Nat. Genet. 16*, 212−213.
8. Fleming, R. J., Scottgale, T. N., Diederich, R. J., and Artavanis-Tsakonas, S. (1990) *Genes Dev. 4*, 2188−2201.
9. Panin, V. M., and Irvine, K. D. (1998) *Semin. Cell Dev. Biol. 9*, 609−617.
10. Greenwald, I. (1998) *Genes Dev. 12*, 1751−1762.
11. Wharton, K. A., Johansen, K. M., Xu, T., and Artavanis-Tsakonas, S. (1985) *Cell 43*, 567−581.
12. Kidd, S., Kelley, M. R., and Young, M. W. (1986) *Mol. Cell. Biol. 6*, 3094−3108.
13. Henderson, S. T., Gao, D., Lambie, E. J., and Kimble, J. (1994) *Development 120*, 2913−2924.
14. Tax, F. E., Yeargers, J. J., and Thomas, J. H. (1994) *Nature 368*, 150−154.
15. Rebay, I., Fleming, R. J., Fehon, R. G., Cherbas, L., Cherbas, P., and Artavanis-Tsakonas, S. (1991) *Cell 67*, 687−699.
16. Jarriault, S., Brou, C., Logeat, F., Schroeter, E. H., Kopan, R., and Israel, A. (1995) *Nature 377*, 355−358.
17. Struhl, G., and Adachi, A. (1998) *Cell 93*, 649−660.
18. De Strooper, B., Annaert, W., Cupers, P., Saftig, P., Craessaerts, K., Mumm, J. S., Schroeter, E. H., Schrijvers, V., Wolfe, M. S., Ray, W. J., Goate, A., and Kopan, R. (1999) *Nature 398*, 518−522.
19. Struhl, G., and Greenwald, I. (1999) *Nature 398*, 522−525.
20. Ye, Y., Lukinova, N., and Fortini, M. E. (1999) *Nature 398*, 525−529.
21. Rand, M. D., Grimm, L. M., Artavanis-Tsakonas, S., Patriub, V., Blacklow, S. C., Sklar, J., and Aster, J. C. (2000) *Mol. Cell. Biol. 20*, 1825−1835.
22. Fleming, R. J. (1998) *Semin. Cell Dev. Biol. 9*, 599−607.
23. Tamura, K., Taniguchi, Y., Minoguchi, S., Sakai, T., Tun, T., Furukawa, T., and Honjo, T. (1995) *Curr. Biol. 5*, 1416−1423.
24. Matsuno, K., Go, M. J., Sun, X., Eastman, D. S., and Artavanis-Tsakonas, S. (1997) *Development 124*, 4265−4273.
25. Matsuno, K., Diederich, R. J., Go, M. J., Blaumueller, C. M., and Artavanis-Tsakonas, S. (1995) *Development 121*, 2633−2644.
26. Zhou, S., Fujimuro, M., Hsieh, J. J., Chen, L., Miyamoto, A., Weinmaster, G., and Hayward, S. D. (2000) *Mol. Cell. Biol. 20*, 2400−2410.
27. Hubbard, E. J., Dong, Q., and Greenwald, I. (1996) *Science 273*, 112−115.
28. Doyle, T. G., Wen, C., and Greenwald, I. (2000) *Proc. Natl. Acad. Sci. U.S.A. 97*, 7877−7881.
29. Petcherski, A. G., and Kimble, J. (2000) *Nature 405*, 364−368.
30. Breeden, L., and Nasmyth, K. (1987) *Nature 329*, 651−654.
31. Bork, P. (1993) *Proteins: Struct., Funct., Genet. 17*, 363−374.
32. Roehl, H., and Kimble, J. (1993) *Nature 364*, 632−635.
33. Sedgwick, S. G., and Smerdon, S. J. (1999) *Trends Biochem. Sci. 24*, 311−316.
34. Batchelor, A. H., Piper, D. E., de la Brousse, F. C., McKnight, S. L., and Wolberger, C. (1998) *Science 279*, 1037−1041.
35. Foord, R., Taylor, I. A., Sedgwick, S. G., and Smerdon, S. J. (1999) *Nat. Struct. Biol. 6*, 157−165.
36. Gorina, S., and Pavletich, N. P. (1996) *Science 274*, 1001−1005.
37. Huxford, T., Huang, D. B., Malek, S., and Ghosh, G. (1998) *Cell 95*, 759−770.
38. Jacobs, M. D., and Harrison, S. C. (1998) *Cell 95*, 749−758.
39. Luh, F. Y., Archer, S. J., Domaille, P. J., Smith, B. O., Owen, D., Brotherton, D. H., Raine, A. R., Xu, X., Brizuela, L., Brenner, S. L., and Laue, E. D. (1997) *Nature 389*, 999−1003.
40. Mandiyan, V., Andreev, J., Schlessinger, J., and Hubbard, S. R. (1999) *EMBO J. 18*, 6890−6898.
41. Russo, A. A., Tong, L., Lee, J. O., Jeffrey, P. D., and Pavletich, N. P. (1998) *Nature 395*, 237−243.
42. Venkataramani, R., Swaminathan, K., and Marmorstein, R. (1998) *Nat. Struct. Biol. 5*, 74−81.
43. Yang, Y., Rao, N. S., Walker, E., Sen, S., and Qin, J. (1997) *Protein Sci. 6*, 1347−1351.
44. Zhang, B., and Peng, Z. (2000) *J. Mol. Biol. 299*, 1121−1132.
45. Zweifel, M. E., and Barrick, D. (2001) *Biochemistry 40*, 14357−14367.

46. Roehl, H., Bosenberg, M., Blelloch, R., and Kimble, J. (1996) *EMBO J. 15*, 7002−7012.
47. Kurooka, H., Kuroda, K., and Honjo, T. (1998) *Nucleic Acids Res. 26*, 5448−5455.
48. Sambrook, J., Fritsch, E. F., and Maniatis, T. (1989) *Molecular Cloning: A Laboratory Manual*, 2nd ed., Cold Spring Harbor Laboratory Press, Plainview, NY.
49. Edelhoch, H. (1967) *Biochemistry 6*, 1948−1954.
50. Eftink, M. R., and Ghiron, C. A. (1981) *Anal. Biochem. 114*, 199−227.
51. Lakowicz, J. R. (1999) *Principles of Fluorescence Spectroscopy*, 2nd ed., Kluwer Academic/Plenum Publishers, New York.
52. Johnson, M. L., Correia, J. J., Yphantis, D. A., and Halvorson, H. R. (1981) *Biophys. J. 36*, 575−588.
53. Stafford, W. F., III (1992) *Anal. Biochem. 203*, 295−301.
54. Stafford, W. F., III (1992) in *Analytical Ultracentrifugation in Biochemistry and Polymer Science* (Harding, S. E., Rowe, A. J., and Horton, J. C., Eds.) pp 359−393, Royal Society of Chemistry, Cambridge, England.
55. Correia, J. J. (2000) *Methods Enzymol. 321*, 81−100.
56. Philo, J. S. (1994) in *Modern Analytical Ultracentrifugation*, pp 156−170, Virkhauser Publishing Co., Boston.
57. Philo, J. S. (1997) *Biophys. J. 72*, 435−444.
58. Cohn, E. J., and Edsall, J. T. (1943) in *Proteins, Amino Acids, and Peptides as Ions and Dipolar Ions*, p 157, Rheinhold, New York.
59. Laue, T. M., Shah, B. D., Ridgeway, T. M., and Pelletier, S. L. (1992) in *Analytical Ultracentrifugation in Biochemistry and Polymer Science* (Harding, S. E., Rowe, A. J., and Horton, J. C., Eds.) Royal Society of Chemistry, Cambridge, England.
60. Tanford, C. (1961) *Physical Chemistry of Macromolecules*, John Wiley & Sons, Inc., New York.
61. Cantor, C. R., and Schimmel, P. R. (1980) *Biophysical Chemistry Part II: Techniques for the study of biological structure and function*, W. H. Freeman and Company, New York.
62. Carrasco, B., and Garcia de la Torre, J. (1999) *Biophys. J. 76*, 3044−3057.
63. Garcia De La Torre, J., Huertas, M. L., and Carrasco, B. (2000) *Biophys. J. 78*, 719−730.
64. Lux, S. E., John, K. M., and Bennett, V. (1990) *Nature 344*, 36−42.
65. Bateman, A., Birney, E., Durbin, R., Eddy, S. R., Howe, K. L., and Sonnhammer, E. L. (2000) *Nucleic Acids Res. 28*, 263−266.
66. Chothia, C., Levitt, M., and Richardson, D. (1981) *J. Mol. Biol. 145*, 215−250.
67. Eftink, M. R., and Ghiron, C. A. (1981) *Arch. Biochem. Biophys. 209*, 706−709.
68. Kuntz, I. D. (1971) *J. Am. Chem. Soc. 93*, 514.
69. Chen, Y. H., Yang, J. T., and Chau, K. H. (1974) *Biochemistry 13*, 3350−3359.
70. Scholtz, J. M., Qian, H., York, E. J., Stewart, J. M., and Baldwin, R. L. (1991) *Biopolymers 31*, 1463−1470.
71. Madison, V., and Schellman, J. (1972) *Biopolymers 11*, 1041−1076.
72. Boice, J. A., and Fairman, R. (1996) *Protein Sci. 5*, 1776−1784.
73. Gay, N. J., and Ntwasa, M. (1993) *FEBS Lett. 335*, 155−160.
74. Michaely, P., and Bennett, V. (1993) *J. Biol. Chem. 268*, 22703−22709.
75. Tang, K. S., Guralnick, B. J., Wang, W. K., Fersht, A. R., and Itzhaki, L. S. (1999) *J. Mol. Biol. 285*, 1869−1886.
76. Byeon, I. J., Li, J., Ericson, K., Selby, T. L., Tevelev, A., Kim, H. J., O'Maille, P., and Tsai, M. D. (1998) *Mol. Cells 1*, 421−431.
77. Sreerama, N., and Woody, R. W. (2000) in *Circular Dichroism. Principles and Applications* (Berova, N., Nakanishi, K., and Woody, R. W., Eds.) Wiley-VCH, New York.
78. Wu, H., Maciejewski, M. W., Marintchev, A., Benashski, S. E., Mullen, G. P., and King, S. M. (2000) *Nat. Struct. Biol. 7*, 575−579.
79. Rice, L. M., and Brunger, A. T. (1999) *Mol. Cells 4*, 85−95.
80. Wolfram, S. (1988) Wolfram Research, Inc., Champaign.

BI011435H